Questions / Keep in Mind

→ T-type Ca^{2+} channel: shift/scale gating variables? Currently shifted/scaled only two parameters based on fit on data.

→ Search for pacemaker neurons in drosophila. Which neurons do they project to? (R5?) Are they inhibitory, or excitatory? Inhibitory will be like a sugar on top :)

→ What is the timescale of Ca^{2+} spikes? Googling resulted in similar shape.

Contents

1 Introduction

- We predict that I_T should provide the inward current for the generation of low-threshold Ca^{2+} spikes, with rapidly activating and inactivating K^+ current I_A modulating the initial components of these Ca^{2+} spikes. In contrast, the slower kinetics of activation and inactivation of the K^+ current I_{K2} suggest that this current may affect more the later portions of low-threshold Ca^{2+} spikes. The properties of I_h suggest that it is critical to modulation of the voltage-time course of the cell at hyperpolarized membrane potentials and may provide a "pacemaker" potential for rhythmic burst generation [8].

- these currents include I_T, the low-threshold, transient Ca^{2+} current that underlines burst firing; the rapidly inactivating and transient K^+ current, I_A, which may fascilitate slow repetitive firing and may interact with I_T during Ca^{2+}-dependent burst firing; a slowly inactivating transient K^+ current, I_{K2}, which may control repetitive firing rate; and a

hyperpolarization-activated, mixed cationic conductance with slow kinetics, I_h, which activates on hyperpolarization and which may generate a "pacemaker" potential for the generation of slow oscillations [8].

- The modeled currents were derived wither from Drosophila neurons (specify), or (e.g. rat thalamic neurons, etc)...

- We assumed that I_T was composed of a uniform populatio of channels whose inactivation could be ompletely described by the Boltzmann function.

- Current-Voltage relationship was better reproduced when constant-field equation was used instead of the ohmic one [8].

- T-Type: $m^3 h$ format [17]

- Model: slow deinactivation [17]

- T-Type Ca current together with the leakage current suffices to describe the low-threshold spike (LTS)... Outward currents are not required to reproduce the basic shape of the LTS... Each LTS trigerres a burst of fast action potentials that ride on its crest. As such, LTS plays a critical role in linking synaptic input to intrinsic membrane mechanisms of bursting in the relay cell and in supporting the slow membrane oscillations underlying the spondling rhythm [17].

- I_T is de-inactivated by hyperpolarization, thus providing an ionic basis for the so-called post-inhibitory rebound excitation [18].

- This "3 Hz" bursting is primarily due to the interplay between a T-type calcium current I_T, and a non-specific cation "sag" current I_h which has much slower kinetics thatn I_T and is activated by hyperpolarization [18].

- Physiologists have been interested in the action of calcium on excitable tissues since the days of Ringer (1883). Some of the main facts established (see Brink, 1954) are that increasing the external calcium concentration raises the threshold, increases membrane resistance (Cole, 1949) and accelerates accommodation. Reducing the calcium concentration has the converse effects, and frequently leads to spontaneous oscillations or repetitive activity (e.g. Adrian & Gelfan, 1933; Arvanitaki, 1939). Other observations which may be less well known are that removal of calcium reduces rectification (Loligo nerve, Steinbach, Spiegelman & Kawata, 1944) and increases the fraction of the sodium carrying system which is in a refractory or inactive condition (Purkinje fibres, Weidmann, 1955). In connexion with the last observation, it is interesting that tissues which do not normally give an anode break response can be made to do so by reducing the concentration of calcium ions in the external medium (Frankenhaeuser, 1957) [5].

2 T-Type Calcium Channel

Contents

2.1 Model

T-Type Ca^{2+} current was modelled using constant-field equation [8]:

$$I_T(V) = m_T(V)^3 h_T(V) P z^2 \frac{VF^2}{RT} \frac{[Ca^{2+}]_{\text{inside}} - [Ca^{2+}]_{\text{outside}} \exp\left[-zFV/(RT)\right]}{1 - \exp\left[-zFV/(RT)\right]} \quad (1)$$

where m_T and h_T correspond to the activation and inactivation gates, P is the maximum permeability (scaled to either have the current amplitude observed during the electrophysiological experiments reported in [11] (Section 2.3), or to), z is the valence of ion (= 2 for Ca^{2+}), V is membrane potential in Volts, F is Faraday's constant ($\approx 9.6485 \times 10^4 C \cdot \text{mol}^{-1}$), R is the universal gas constant ($\approx 8.3145 J/K^\circ \cdot \text{Mol}$), T is temperature is Kelvin (here, $273.16 + 25 = 298.16^\circ$). $[Ca^{2+}]_{\text{inside}}$ and $[Ca^{2+}]_{\text{outside}}$ are the concentrations of Ca^{2+} inside and outside the membrane. The values were set to $23 \times e^{-9}$ and $0.5 \times e^{-3}$ correspondingly, from the motor neurons in Drosophila [5].

Another approach to model the T-Type Ca^{2+} current is by Ohm's law [8, 17]:

$$I_T(V) = g_T m_T(V)^3 h_T(V)(V - V_{Ca}) \quad (2)$$

g_T is the maximum value of the conductance of the T-Type Ca^{2+} current, and V_{Ca} us the reversal potential for Ca^{2+}, which can be estimated given the ion concentrations inside and outside the membrane (see Section 2.1.1). However, the model with the Ohmic current did not reproduce the I-V relations in [11] correctly (see Sction ...). Similar issue was described in [8], where choosing equation 1 instead of 2 resulted in better fit of the I-V relationship to the experimental data.

2.1.1 Reversal Potential

Reversal potential was estimated by Nernst equation [10]:

$$V_{\text{ion}} = \frac{RT}{zF} \ln \frac{[\text{Ion}]_{\text{outside}}}{[\text{Ion}]_{\text{inside}}}$$

where $[\text{Ion}]_{\text{inside}}$, and $[\text{Ion}]_{\text{outside}}$ are concentrations of the ions (here, Ca^{2+}) inside and outside of the cell. The values for $[Ca^{2+}]_{inside}$ and $[Ca^{2+}]_{outside}$ were taken to be $23nM$, and $0.5mM$ correspondingly from the motor neurons in Drosophila [14]. R is the universal gas constant ($\approx 8.3145 J/K^\circ \cdot \text{Mol}$), T is temperature is Kelvin (here, $273.16 + 25 = 298.16^\circ$), F is Faraday's constant ($\approx 9.6485 \times 10^4 C \cdot \text{mol}^{-1}$), z is the valence of the ion ($z = 2$ for Ca^{2+}).

$$V_{Ca} \approx 128mV$$

2.1.2   Activation Gate

Dynamics of the activation variable m_T of T-Type Ca^{2+} channel is given by [17]:

$$\frac{dm_T(V)}{dt} = \frac{m_{T,\infty}(V) - m_T(V)}{\tau_{m_T}(V)}$$

where [2, 17]:

$$m_{T,\infty}(V) = \frac{1}{1 + \exp\left[-(V - V_{m_T,1/2})/k_{m_T}\right]} \tag{3}$$

and

$$\tau_{m_T}(V) = \sigma_{m_T}(V)\tau_{m_T}^-(V) + (1 - \sigma_{m_T}(V))\tau_{m_T}^+(V) \tag{4}$$

In the equations above, $m_{T,\infty}$ and τ_{m_T} are voltage-sensitive steady-state activation function and time constant, correspondingly. $V_{m_T,1/2}$ is membrane potential at which the steady-state activation function is equal to its half-maximum (i.e. 0.5), and k_{m_T} is the slope factor. $\tau_{m_T}^-(V)$ and $\tau_{m_T}^+(V)$ describe the time constant below (deactivation) and above (activation) -50mV correspondingly, and $\sigma_{m_T}(V)$ defines smooth transition between the two at -50mV. First, the following functions were fit to the values provided in [11]:

$$\tau_{m_T}^-(V) = 3(a_{m_T,1} + \exp\left[(V - b_{m_T,1})/k_{m_T,1}\right]) \tag{5}$$
$$\tau_{m_T}^+(V) = a_{m_T,2} + \exp\left[-(V - b_{m_T,2})/k_{m_T,2}\right] \tag{6}$$

The scaling factor 3 for $\tau_{m_T}^-(V)$ is related to the how deactivation time constant was measured in [11] (for the details see Section 2.2.2). As the equations 5 have discontinuity at $V = -50$mV, after fitting the parameters of those equations, the following equation for $\sigma_{m_T}(V)$ was chosen to model smooth transition between the two:

$$\sigma_{m_T}(V) = \frac{1}{1 + \exp\left[c_{\tau_{m,T}}(v + 50)\right]} \tag{7}$$

where $c_{\tau_{m,T}} > 0$ controls the sharpness of the transition and was fitted to the combined activation and deactivation time constants from [11] after fixing the parameters of equation 5.

2.1.3   Inactivation Gate

Inactivation gate was modelled with first-order kinetic scheme [3, 4]:

$$\frac{dh_T(V)}{dt} = \frac{h_{T,\infty}(V) - h(V)}{\tau_{h_T}(V)}$$

where [3, 17]:

$$h_{T,\infty}(V) = \frac{1}{1 + \exp\left[(V - V_{h_T,1/2})/k_{h_T}\right]} \tag{8}$$

and [18]:

$$\tau_{h_T}(V) = h_{T,\infty}(V)(a_{h_T} + \exp\left[(V - b_{h_T})/k_{h_T}\right]) \tag{9}$$

Note 1. Second order kinetic schemes have also been developed for the inactivation gates [17]. The derivation of the equations in the paper are provided in more detail in Section 2.4.3.

2.2 Fitting Data

As the data from the article is not available online, the values were estimated by taking screenshot, importing the image in Coreldraw and estimating the values using visual inspection and coordinate system of Coreldraw. The fitting was performed using python function *scipy.optimize.curve_fit*. The following plots show the estimated activation/inactivation variables, as well as time constants as a function of test potential V, as provided in [11]:

Note 2. The error due to the subjective visual inspection should not be large. I did not estimated the error, but with moving the manually placed dot over the image on the did not have considerable effect in the final values (within the moving range where the manually placed dots were not obviously not overlapping with the ones from the image).
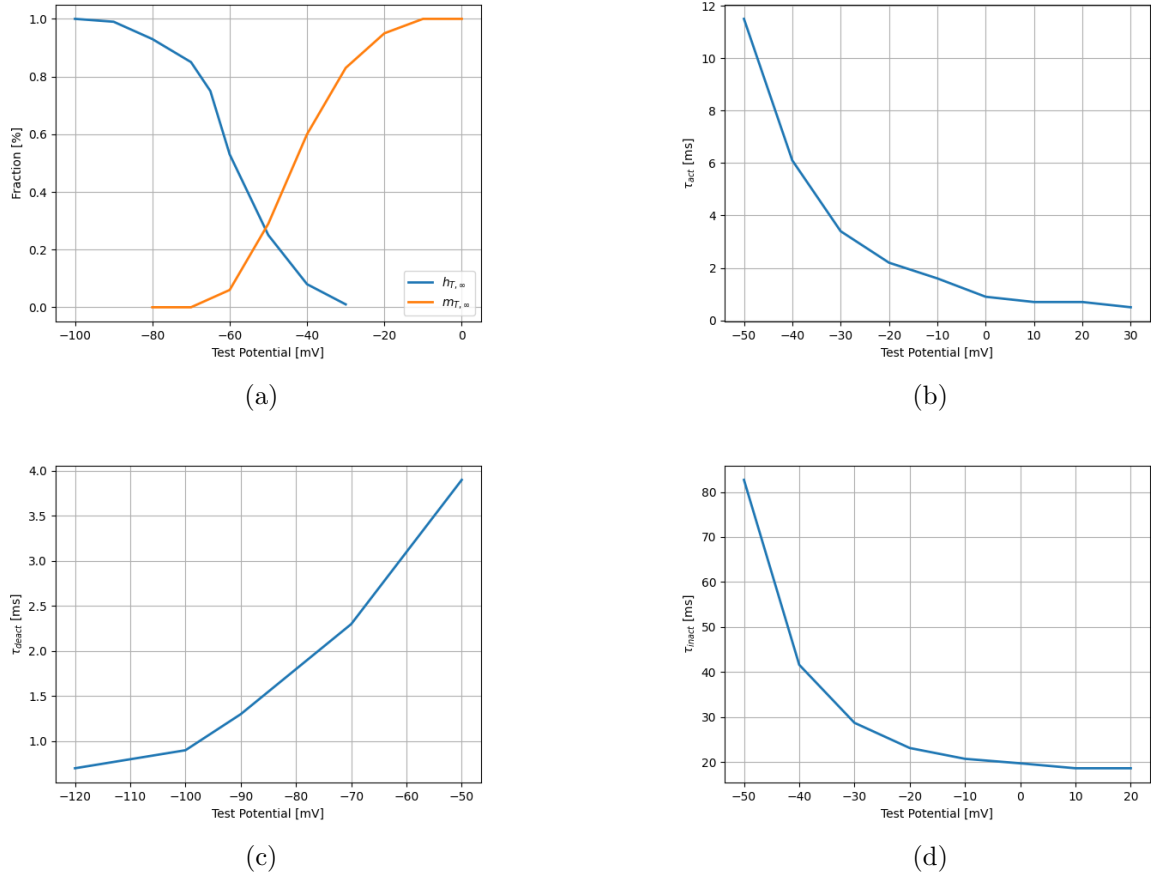

Figure 1: (a) Steady-state activation and inactivation functions of T-type Ca^{2+} channel; (b) Activation, (b) deactivation and (c) inactivation as a functions of test potentials. Data adapted from [11].

The values of the resulted estimates (plotted in the figures above) are provided in Section 2.4.1.

2.2.1 Estimating Steady-State Activation/Inactivation Function

Parameters for steady-state activation variable were estimated by fitting $m_{T,\infty}^3(V)$ (see Equation 3) to the data from electrophysiological recordings presented in [11] (similar to the procedure described in [2]). The steady-state inactivation was estimated by fitting Equation 8 to the data from the same paper.
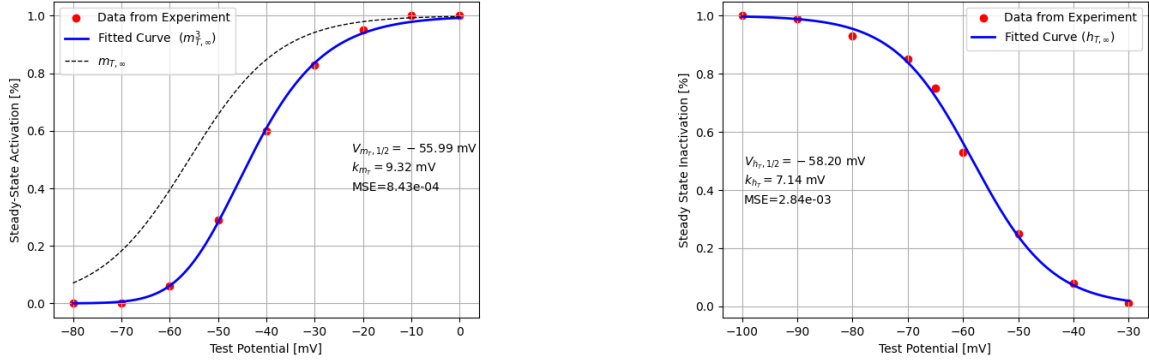

Figure 2: Fitted data to [11].

2.2.2 Estimating Activation/Inactivation Time Constants

The data was taken from [11]. The paper provides information about the values for activation/inactivation variables, as well as time constants as a functions of membrane potentials.

Activation time constant

$a_{T,1}$, $b_{T,1}$, $k_{T,1}$, $a_{T,2}$, $b_{T,2}$, $k_{T,2}$ parameters were fit to the activation ($V \geq -50$ mV) and deactivation ($V < -50$ mV) time constants provided in [11] (equations 5). The initial guess for the parameters were chosen to be 0, -120, 1 for $a_{T,1}$, $b_{T,1}$, $k_{T,1}$, and 0, 50, 1 for $a_{T,2}$, $b_{T,2}$, $k_{T,2}$, correspondingly. The results are shown in Figure 3a.

[11] estimated the activation time constant ($V > -50$ mV) by fitting sum of two exponentials to the recorded current trace. As it is shown in Section 2.4.2, the fitted time constant does not need adjustment to account for the correspondingly time constant of activation. However, the deactivation time constant needs an adjustment.

The authors estimated deactivation time constant by measuring decay of the tail current (τ_{tail}). As the model consists of three activation gates, and closing of each ion channel reuires only one activation gate to close, the deactivation time constant for one gate (out of the three) will be three times as large as τ_{tail} [8]. For this reason, τ_{m_t} for $V < -50$ mV was determined as $3 \times \tau_{\text{tail}}$.

As the set of equations 5 have jump discontinuity at $V = -50$mV, σ_{m_T} was introduced to model a smooth transition between the functions describing the time constant below and above -50mV (equation 7). The parameters of the exponentials modelling activation and deactivation time constants were fixed, and the parameter $c_{\tau_m,T}$ of σ_{m_T} was fitted to the combined data of activation and deactivation time constants from [11] (Figure 3b).

Note 3. Original paper for the base model of the R5 neuron [18] did not model the activation time constant of T-Type Ca^{2+} channels, as they replaced the activation variable by its steady state equation $m_{t,\infty}(V)$.

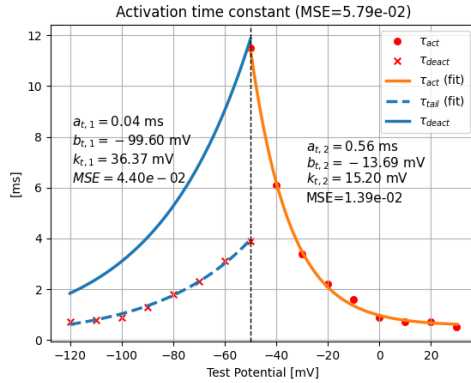**Note 4.** [3] fitted activation time constant to double exponentials:

$$\tau_{m_T} = a_{\tau_{m_T}} + \frac{b_{\tau_{m_T}}}{\exp\left[(V - V_{\tau_{m_T}^1,1/2})/k_{\tau_{m_T}^1}\right] + \exp\left[-(V - V_{\tau_{m_T}^2,1/2})/k_{\tau_{m_T}^2}\right]} \tag{10}$$

However, MSE in case of double exponential fit was larger than with fitting the activation time constant with two exponential (see Fig.), as described above.
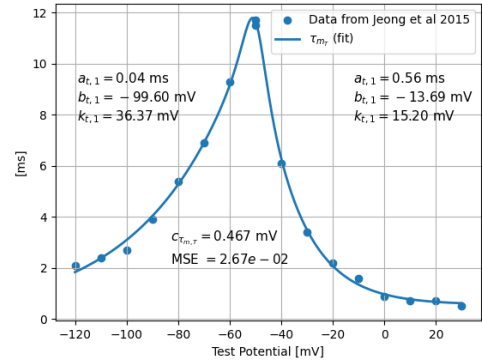
Inactivation time constant

[11] did not provide experimental values for τ_{h_T} below -50mV. Several authors reported recovery time constant for deinactivation to be much slower than the one of inactivation [3, 8, 9]. Equation 9 is a negative sigmoid, with a left asymtote at $V \approx 216$mV (Figure 4).

Note 5. Another approach would be to fit the time constant only above -50mV and take values below -50mV from another source (e.g. [8]). However, as 1) the values for Drosophila T-Type channel are not available below -50mV, 2) the fitted time constant has the same order of magnitude below -50mV as described in the literature for deinactivation time constant, 3) given the previous comment, the exact velues will only affect time course of the current and is not very relevant for the neuronal model - continuous function was preferred for modelling the inactivation time constant.

(a) Fitted activation and deactivation time constants using exponential functions

(b) Smooth transition between activation and deactivation time constants

Figure 3: Fitted τ_{m_T} to data from [11].
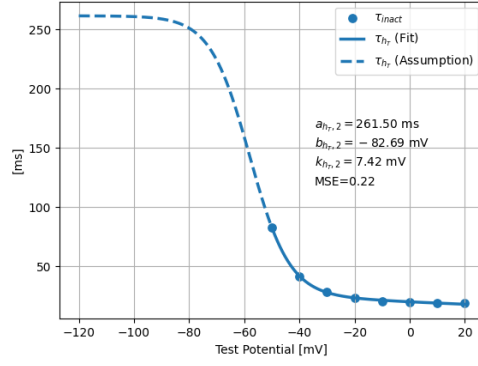
Figure 4: Fitted inactivation time constant

2.3 Simulations of T-Type Ca^{2+} Current

Simulations were done using python package '*scipy.integrate.solve_ivp*' with zero initial conditions. Different integration methods were compared: RK45, BDF, and LSODA. Each solver is optimized for different problems (stiff, non-stiff, etc.). Simulations showed, that for some cases (e.g. simulating only t-type channel) it is best to use RK45. For the simulatins presented in this section, RK45 method was used.

2.3.1 Ohmic Current vs Constant-Field Equation

Add text, add captions in figure 6.
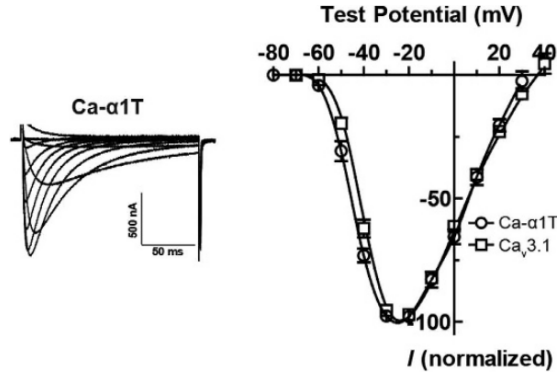
Figure 5: I-V relationship of T-Type Ca^{2+} current in Drosophila. Adapted from [11].

9
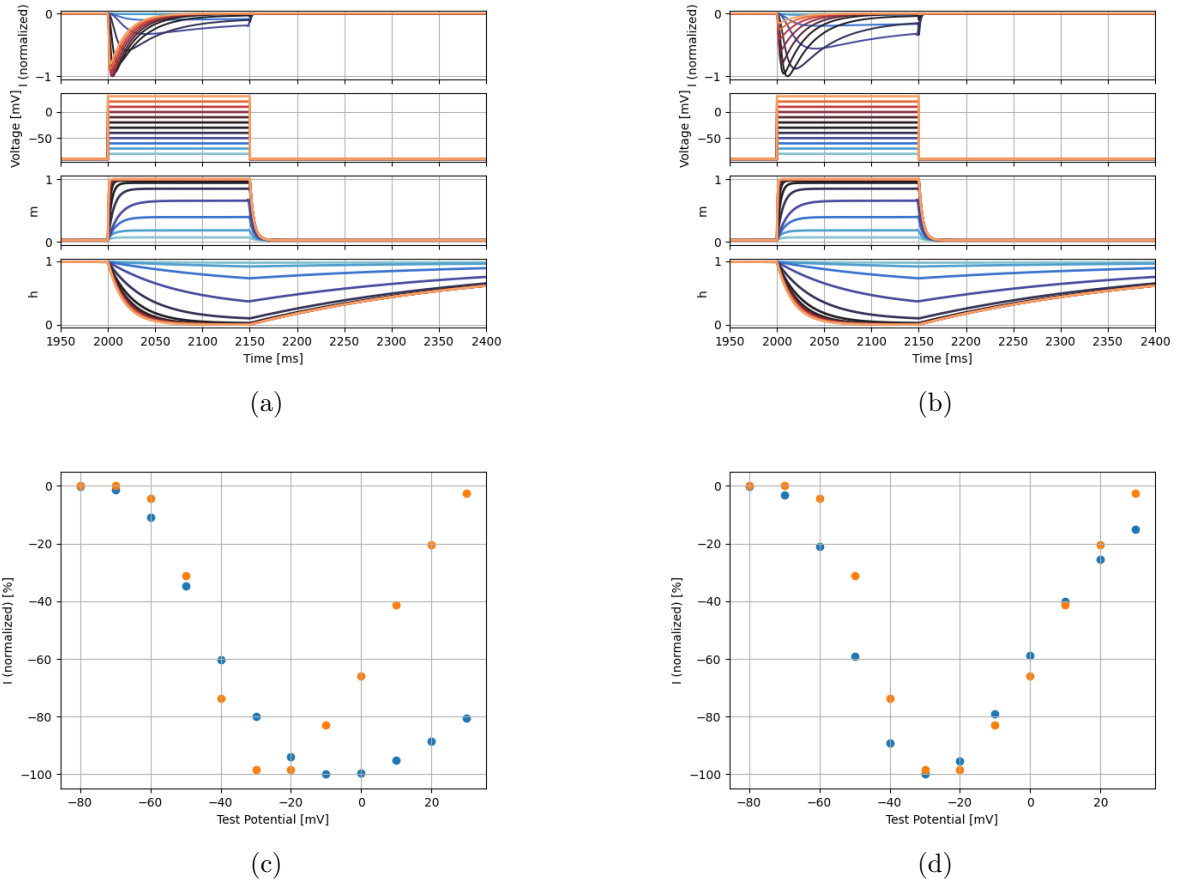
Figure 6: Ohm's low vs constant-field equation for T-Type Ca^{2+} current.

2.3.2 Scaling/Shifting Gating Variables

- $[Ca]_{outside}$ affects gating constants.

- Shifted steady state activation and scaled tau activation (python function curve_fit with initial guesses p0=[4, 0.5] for shift and scale correspondingly)

- m(v) to m(v-4.95)

- tau to tau*0.45

Figure 7: Add Text

Figure 8: Add Text

2.4 Appendix

2.4.1 Estimates of Data in Jeong et al 2015

Inactivation

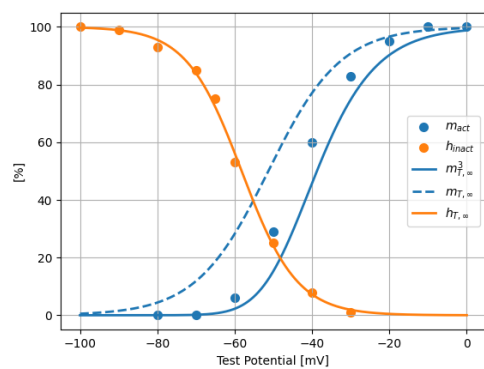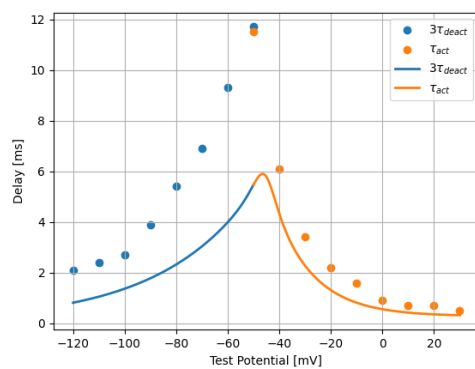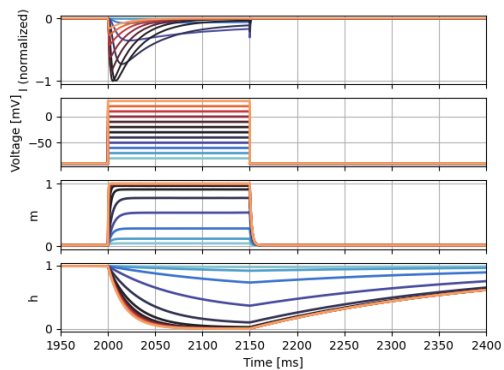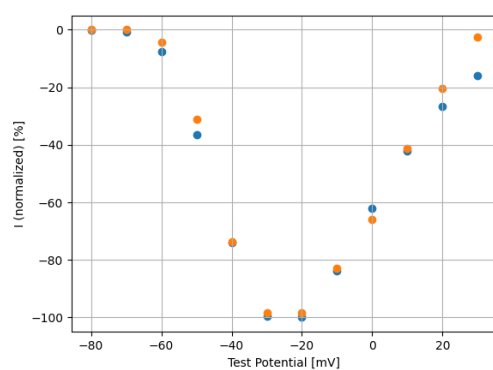| Length	y1	y2	Perc	Round	Test Potential
84.347	138.308	222.656	1.000011856	1	-100
84.347	138.308	221.91	0.9911674393	0.99	-70
84.347	138.308	216.864	0.931343142	0.93	-80
84.347	138.308	210.296	0.8534743382	0.85	-70
84.347	138.308	201.258	0.7463217423	0.75	-65
84.347	138.308	183.423	0.5348737952	0.53	-60
84.347	138.308	159.321	0.2491256358	0.25	-50
84.347	138.308	145.041	0.0798250086	0.08	-40
84.347	138.308	139.015	0.008382040855	0.01	-30

Activation

Length	y1	y2	Perc	Round	Test Potential
84.347	138.308	138.308	0	0	-80
84.347	138.308	138.308	0	0	-70
84.347	138.308	143.029	0.05597116673	0.06	-60
84.347	138.308	162.76	0.2898976846	0.29	-50
84.347	138.308	189.012	0.6011357843	0.6	-40
84.347	138.308	208.417	0.8311973159	0.83	-30
84.347	138.308	218.852	0.954912445	0.95	-20
84.347	138.308	222.256	0.9952695413	1	-10
84.347	138.308	222.656	1.000011856	1	0

Tau Activation

Test Potential	length	k	y1	y2	Tau	Round
-50	94.853	10	110.837	220.142	11.52362076	11.5
-40	94.853	10	110.837	168.638	6.093745058	6.1
-30	94.853	10	110.837	143.507	3.444276934	3.4
-20	94.853	10	110.837	131.792	2.209207932	2.2
-10	94.853	10	110.837	126.028	1.60153079	1.6
0	94.853	10	110.837	119.373	0.8999188218	0.9
10	94.853	10	110.837	117.386	0.6904367811	0.7
20	94.853	10	110.837	117.187	0.6694569492	0.7
30	94.853	10	110.837	115.995	0.5437888101	0.5

Tau Inactivation

Test Potential	length	k	y1	y2	Tau	Round
-50	122.173	100	120.28	221.365	82.73923044	82.7
-40	122.173	100	120.28	171.102	41.59838917	41.6
-30	122.173	100	120.28	155.338	28.69537459	28.7
-20	122.173	100	120.28	148.484	23.08529708	23.1
-10	122.173	100	120.28	145.514	20.65431806	20.7
0	122.173	100	120.28	144.372	19.71957798	19.7
10	122.173	100	120.28	143.001	18.59739877	18.6
20	122.173	100	120.28	143.001	18.59739877	18.6

Tau Deactivation

Test Potential	length	k	y1	y2	Tau	Round
-120	130.684	5	125.975	143.595	0.6741452664	0.7
-110	130.684	5	125.975	146.32	0.7784043953	0.8
-100	130.684	5	125.975	149.948	0.9172125126	0.9
-90	130.684	5	125.975	158.758	1.254285146	1.3
-80	130.684	5	125.975	173.788	1.829336415	1.8
-70	130.684	5	125.975	186.399	2.311836185	2.3
-60	130.684	5	125.975	206.439	3.07857121	3.1
-50	130.684	5	125.975	227.86	3.898143614	3.9

2.4.2 From Current Trace to Sum of Exponentials

Sum of exponentials and gating time constants

$$\frac{dm}{dt} = \frac{m_\infty - m}{\tau_m} \quad ; \quad \frac{dh}{dt} = \frac{h_\infty - h}{\tau_h} \qquad (1)$$

$$I(t) = g\, m^p\, h\, (V - E) \qquad (2)$$

$$m(0) = h(0) = 0 \;\Big)\Rightarrow \quad m(t) = m_\infty \left(1 - e^{-t/\tau_m}\right)$$
$$P = 3 \qquad\qquad\qquad h(t) = h_\infty \left(1 - e^{-t/\tau_h}\right) \Bigg) \Rightarrow$$
$$(2)$$

$$\Rightarrow\; I(t) = g\, m_\infty^3 \left(1 - e^{-t/\tau_m}\right)^3 h_\infty \left(1 - e^{-t/\tau_h}\right)(V - E) =$$

$$= g\, m_\infty^3 \left(1 - e^{-3t/\tau_m} - 3e^{-t/\tau_m} + 3e^{-2t/\tau_m}\right) h_\infty \left(1 - e^{-t/\tau_h}\right)(V-E) \simeq$$

$$\simeq g\, m_\infty^3 \left(1 - 3e^{-t/\tau_m}\right) h_\infty \left(1 - e^{-t/\tau_h}\right)(V - E) =$$

$$= g\, m_\infty^3 h_\infty \left(1 - e^{-t/\tau_h} - 3e^{-t/\tau_m} + e^{-t/\tau_m - t/\tau_h}\right)(V - E) \simeq$$

$$\simeq g\, m_\infty^3 h_\infty \left(1 - e^{-t/\tau_h} - 3e^{-t/\tau_m}\right)(V - E) =$$

$$= \underbrace{g\, m_\infty^3 h_\infty (V - E)}_{\text{Steady state term}} \underbrace{- g\, m_\infty^3 h_\infty (V-E)\, e^{-t/\tau_h} - 3g\, m_\infty^3 h_\infty (V-E)\, e^{-t/\tau_m}}_{\text{Transient term}}$$

$$I_{transient}(t) = A_1\, e^{-t/\tau_m} + A_2\, e^{-t/\tau_h}$$

$$A_1 = -3\, g\, m_\infty^3 h_\infty (V - E)$$

$$A_2 = - g\, m_\infty^3 h_\infty (V - E)$$

← Thus, τ_m and τ_h can be directly fitted by recorded transient currents $I_{transient}$

2.4.3 Derivation of equations in Wang 1991

$$\frac{dh}{dt} = d_1(1-h-d) - \beta_2 h \quad (1)$$

$$\frac{dd}{dt} = \beta_2(1-h-d) - d_2 d \quad (2)$$

steady state

$$d_1(1-h_\infty - d_\infty) = \beta_2 h_\infty \;) \Rightarrow\; d_1(1-d_\infty) = h_\infty(d_1+\beta_1) \;\Rightarrow\; h_\infty = \frac{d_1(1-d_\infty)}{d_1+\beta_1}$$

$$\beta_2(1-h_\infty - d_\infty) = d_2 d_\infty \;) \Rightarrow\; \beta_2\left(1 - \frac{d_1(1-d_\infty)}{d_1+\beta_1} - d_\infty\right) = d_2 d_\infty$$

$$1 - \frac{d_1 - d_1 d_\infty + d_1 d_\infty + \beta_1 d_\infty}{d_1+\beta_1} = \frac{d_2}{\beta_2} d_\infty$$

$$\frac{d_1 + \beta_1 d_\infty}{d_1+\beta_1} = 1 - \frac{d_2}{\beta_2} d_\infty \;) \Rightarrow\; \cancel{d_1} + \beta_1 d_\infty = \cancel{d_1} + \beta_1 - \frac{d_2(d_1+\beta_1)}{\beta_2} d_\infty$$

$$d_\infty\left(\beta_1 + (d_1+\beta_1)\frac{d_2}{\beta_2}\right) = \beta_1$$

$$d_\infty \cdot \frac{\beta_1\beta_2 + d_1 d_2 + d_2\beta_1}{\beta_2} = \beta_1$$

$$\left. \begin{aligned} d_\infty &= \frac{\beta_1\beta_2}{\beta_1\beta_2 + d_2(d_1+\beta_1)} \\[1em] \beta_1 &= d_1 K_1 \\ \beta_2 &= d_2 K_2 \end{aligned} \right) \Rightarrow\; d_\infty = \frac{d_1 K_1\, \cancel{d_2} K_2}{d_1 K_1\, \cancel{d_2} K_2 + \cancel{d_2}\left(d_1 + d_1 K_1\right)} =$$

$$= \frac{\cancel{d_1} K_1 K_2}{\cancel{d_1} K_1 K_2 + \cancel{d_1}(1+K_1)} = \frac{K_1 K_2}{K_1 K_2 + 1 + K_1} = \frac{K_1 K_2}{1 + K_1(1+K_2)}$$

$$h_\infty = \frac{d_1(1-d_\infty)}{d_1 + \beta_1} = \frac{d_1}{d_1 + K_1 d_1}\left(1 - \frac{K_1 K_2}{1 + K_1 + K_1 K_2}\right) =$$

$$= \frac{1}{1+K_1} \cdot \frac{1 + K_1 + K_1 K_2 - K_1 K_2}{1 + K_1 + K_1 K_2} = \frac{1}{1+K_1} \cdot \frac{1+K_1}{1 + K_1 + K_1 K_2} =$$

$$= \frac{1}{1 + K_1(1 + K_2)}$$

$$\boxed{\begin{aligned} h_\infty &= \frac{1}{1 + K_1(1 + K_2)} \\ d_\infty &= K_1 K_2\, h_\infty \end{aligned}} \qquad \begin{aligned} &(A2a) \\[1em] &(A2\beta) \end{aligned}$$

$$K_1 = K_2 \Rightarrow \boxed{\begin{aligned} h_\infty &= \frac{1}{1 + K + K^2} \\ d_\infty &= K^2 h_\infty \end{aligned}} \qquad (A3)$$

$$\begin{matrix} (1) \\ (2) \end{matrix} \rightarrow \quad \frac{d}{dt}\begin{pmatrix} h \\ d \end{pmatrix} = \begin{pmatrix} -d_1 - \beta_1 & -d_1 \\ -\beta_2 & -d_2 - \beta_2 \end{pmatrix}\begin{pmatrix} h \\ d \end{pmatrix} + \begin{pmatrix} d_1 \\ \beta_2 \end{pmatrix}$$

Associated homogeneous equation:

$$\frac{d}{dt}\begin{pmatrix} h \\ d \end{pmatrix} = \begin{pmatrix} -d_1 - \beta_1 & -d_1 \\ -\beta_2 & -d_2 - \beta_2 \end{pmatrix}\begin{pmatrix} h \\ d \end{pmatrix}$$

$$\begin{pmatrix} h \\ d \end{pmatrix} \equiv \vec{x}$$

$$\begin{pmatrix} -d_1 - \beta_1 & -d_1 \\ -\beta_2 & -d_2 - \beta_2 \end{pmatrix} \equiv A$$

$$\lambda' = -\lambda \quad \text{2 eigenvalues}$$

$$\vec{x}' = A \, \vec{x}$$

$$\det(A + \lambda I) = \det \begin{pmatrix} -d_1 - \beta_1 + \lambda & -d_1 \\ -\beta_2 & -d_2 - \beta_2 + \lambda \end{pmatrix} =$$

$$= (-d_1 - \beta_1 + \lambda)(-d_2 - \beta_2 + \lambda) - d_1 \beta_2 =$$

$$= d_1 d_2 + d_1 \beta_2 - \lambda d_1 + d_2 \beta_1 + \beta_1 \beta_2 - \lambda \beta_1 - \lambda d_2 - \lambda \beta_2 + \lambda^2 - d_1 \beta_2 =$$

$$= \lambda^2 + \lambda \underbrace{(-d_1 - \beta_1 - d_2 - \beta_2)}_{T_r} + \underbrace{d_1 d_2 + \beta_1(d_2 + \beta_2)}_{D} =$$

$$= \lambda^2 + T_r \cdot \lambda + D$$

$$T_r = -(d_1 + \beta_1 + d_2 + \beta_2) = -\left(\frac{1}{\tau_1} + \frac{1}{\tau_2}\right)$$

$$D = d_1 d_2 + \beta_1(d_2 + \beta_2) = d_1 d_2 + K d_1 (d_2 + K d_2) =$$

$$= d_1 d_2 (1 + K(1 + K))$$

$$K_1 = \frac{\beta_1}{d_1} \;) \Rightarrow \; \beta_1 = K_1 d_1$$

$$\tau_1 = \frac{1}{d_1 + \beta_1} \;) \Rightarrow \tau_1 = \frac{1}{d_1(1 + K_1)} \;) \Rightarrow \; d_1 = \frac{1}{\tau_1(1 + K_1)}$$

$$\text{similarly}: \; d_2 = \frac{1}{\tau_2(1 + K_2)}$$

$$) \Rightarrow \; D = \frac{1 + K(1 + K)}{\tau_1 \tau_2 (1 + K)^2}$$

$$\lambda_1, \lambda_2 = \frac{1}{2}\left[-T_r \pm \sqrt{T_r^2 - 4D} \right]$$

$$T_r^2 - 4D = \left(\frac{1}{\tau_1} + \frac{1}{\tau_2}\right)^2 - \frac{4(1+K(1+K))}{\tau_1 \tau_2 (1+K)^2} =$$

$$= \left(\frac{1}{\tau_1} - \frac{1}{\tau_2}\right)^2 + \frac{4}{\tau_1 \tau_2} - \frac{4(1+K(1+K))}{\tau_1 \tau_2 (1+K)^2} = \left(\frac{1}{\tau_1} - \frac{1}{\tau_2}\right)^2 + \frac{4(1+K)^2 - 4 - 4K - 4K^2}{\tau_1 \tau_2 (1+K)^2} =$$

$$= \left(\frac{1}{\tau_1} - \frac{1}{\tau_2}\right)^2 + \frac{4 + 8K + 4K^2 - 4 - 4K - 4K^2}{\tau_1 \tau_2 (1+K)^2} = \left(\frac{1}{\tau_1} - \frac{1}{\tau_2}\right)^2 + \frac{4K}{\tau_1 \tau_2 (1+K)^2}$$

$$\lambda_1, \lambda_2 = \frac{1}{2}\left[\left(\frac{1}{\tau_1} + \frac{1}{\tau_2}\right) \pm \sqrt{\left(\frac{1}{\tau_1} - \frac{1}{\tau_2}\right)^2 + \frac{4K}{\tau_1 \tau_2 (1+K)^2}} \right]$$

$\downarrow$ (from the paper)

$$\tau_1^{-1}, \tau_2^{-2} = \frac{1}{2}\left[(\lambda_1 + \lambda_2) \pm \sqrt{(\lambda_1 + \lambda_2)^2 - \frac{4(1+K)^2 \lambda_1 \lambda_2}{1 + K(1+K)}} \right]$$

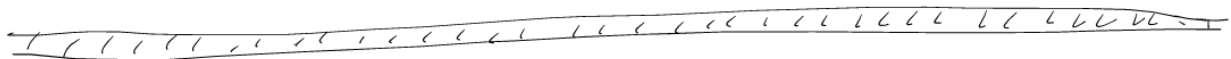Measurable time constants in experiments are λ_1^{-1} and λ_2^{-1} (i.e. $\tilde{\tau}_R$ and $\tilde{\tau}_r$).

general solution for d and h:

$$A_0^{(\ell)} + A_1^{(\ell)} \exp\left(-\lambda_1 t\right) + A_2^{(\ell)} \exp\left(-\lambda_2 t\right)$$

where $\ell = \{d, h\}$

17

Approximations:

$$\tau_1 \simeq \lambda_1^{-1}$$
$$\tau_2 \simeq \lambda_2^{-1}\left[1 + K(1+K)\right]/(1+K)^2$$

$$\dot{h} = d_1(1 - h - d) - \beta_1 h \qquad (1)$$
$$\dot{d} = \beta_2(1 - h - d) - d_2 d \qquad (2)$$

As (1) describes much faster process than (2), the authors used rapid equilibrium hypothesis on the former: assume steady state

$$\frac{dh}{dt} = 0. \quad \text{Then:}$$

$$\left. h = \frac{d_1(1-d)}{d_1 + \beta_1} \right) \Rightarrow$$

$$(2)$$

$$) \Rightarrow \quad \dot{d} = \beta_2\left(1 - \frac{d_1(1-d)}{d_1 + \beta_1} - d\right) - d_2 d =$$

$$= \beta_2 - \frac{d_1 \beta_2 (1-d)}{d_1 + \beta_1} - \beta_2 d - d_2 d =$$

$$= \frac{d_1 \beta_2 + \beta_1 \beta_2 - d_1 \beta_2 + d_1 \beta_2 d - d_1 \beta_2 d - \beta_1 \beta_2 d - d_1 d_2 d - d_2 \beta_1 d}{d_1 + \beta_1} =$$

$$= \frac{d_1 d_2 K^2 (1-d) - d_1 d_2 d - d_1 d_2 K d}{d_1 + \beta_1}$$

$$\dot{d} = \frac{d_1 d_2 K^2 (1-d) - d_1 d_2 d - d_1 d_2 K d}{d_1 + d_1 K} =$$

$$= \frac{d_2 K^2 (1-d) - d_2 d - d_2 K d}{1+K} = \frac{d_2 \left(K^2 - K^2 d - d - K d \right)}{1+K} =$$

$$= \frac{d_2 \left(K^2 - d \left(1 + K(1+K) \right) \right)}{1+K} = -\frac{d_2 \left(1 + K(1+K) \right)}{1+K} d + \frac{d_2 K^2}{1+K} \cdot$$

$$\frac{1+K}{d_2 \left(1 + K(1+K) \right)} \dot{d} = -d + \frac{d_2 K^2}{1+K} \cdot \frac{1+K}{d_2 \left(1 + K(1+K) \right)}$$

$$\frac{1+K}{d_2 \left(1 + K(1+K) \right)} \equiv \lambda_2^{-1}$$

$$\boxed{ \lambda_2^{-1} \dot{d} = -d + \frac{K^2}{1 + K(1+K)} } \qquad (\ast) \qquad d_1 = \frac{1}{\tau_1 (1+K_1)}$$

$$\left. \begin{array}{l} \lambda_2^{-1} = \dfrac{1+K}{d_2 \left(1 + K(1+K) \right)} \\[2em] d_2 = \dfrac{1}{\tau_2 (1+K)} \end{array} \right\} \;\Rightarrow\; \lambda_2^{-1} = \frac{\tilde{\tau}_2 (1+K)^2}{1 + K(1+K)}$$

$$\boxed{ \tau_2 = \frac{\lambda_2^{-1} \left(1 + K(1+K) \right)}{(1+K)^2} }$$

2.4.4   Overcoming Singularities in Constant-Field Equation

$$\boxed{I_T = \hat{g}\, P\, z^2\, \frac{EF^2}{RT}\, \frac{[Ca^{2+}]_i - [Ca^{2+}]_o\, \exp(-zFE/RT)}{1 - \exp(-zFE/RT)}}$$

$$\boxed{\hat{g} = m^3 h}$$

$$\text{if} \quad -\frac{zFE}{RT} \gg 1 \quad) \Rightarrow \quad I_T = \hat{g}\, P\, z^2\, \frac{EF^2}{RT} \cdot \frac{-[Ca^{2+}]_o}{0-1}$$

$$\boxed{I_T = \hat{g}\, P\, z^2\, \frac{EF^2}{RT}[Ca^{2+}]_o}$$

$$\text{if } E = 0 \quad) \Rightarrow \quad I_T \simeq \hat{g}\, P\, z^2\, \frac{EF^2}{RT}\, \frac{[Ca^{2+}]_i - [Ca^{2+}]_o\left(1 - \frac{zFE}{RT}\right)}{1 - \left(1 - \frac{zFE}{RT}\right)} \simeq$$

$$\simeq \hat{g}\, P\, z^2\, \frac{EF^2}{RT}\, \frac{[Ca^{2+}]_i - [Ca^{2+}]_o}{\frac{zFE}{RT}}$$

$$\boxed{I_T = \hat{g}\, P\, z\, F\left([Ca^{2+}]_i - [Ca^{2+}]_o\right)}$$
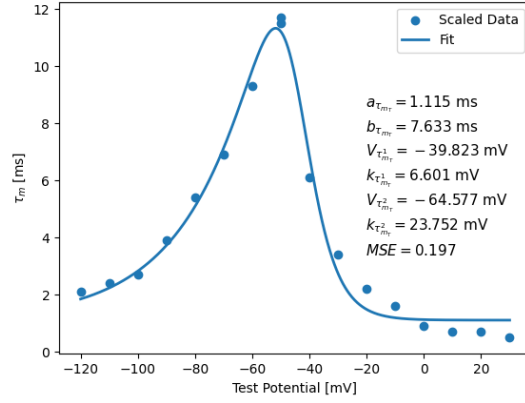
2.4.5 Additional Figures

Figure 9: Fitting time constant of activation function for T-Type Ca^{2+} channel by double exponential function (Eq. 10). The fitting was done using the Python library *scipy.optimize.curve_fit* with the following initial guesses for the parameters: $a_{\tau_{m_T}} = 2$, $b_{\tau_{m_T}} = 1$, $V_{\tau_{m_T}^1} = -100$, $k_{\tau_{m_T}^1} = 10$, $V_{\tau_{m_T}^2} = -40$, $k_{\tau_{m_T}^2} = 10$.

3 Sodium and Potassium Channels

3.1 Sodium Channels

- Drosophila genome has two genes predicted to encode Na_v proteins: para, and 60E (NaCP60E). However, NaCP60E null mutants showed no loss in inward sodium current, suggesting that para is the putative Na_v channel [16].

- para has 60 predicted isoforms via alternative splicing [16]

- Para is only expressed in active neurons [16]

- Currently I chose vales from [19] where $DmNa_v$ was expressed in Xenopus ooscyte (frog). The similar was done in [13], but the values are different.

- "heterologous expression indicates that the inclusion of specific exons imparts characteristic gating properties to individual splice variants of $DmNa_v$ channels. These differences likely contribute to, and may even explain, the diversity in action potential firing between different neurons observed in the Drosophila CNS"

- [16] stated in Fig. 5 that 4th power exponential fit for activation resutled in time constant equal to 2.1. This means, that for one gate it should be 8.4.

The model and parameters for the transient and persistent Na channels, as well as fast and slow K currents were taken from [7]. All currents are modelled according to Ohm's law:

$$I_c(V, m, h) = g_c m_c^{p_c}(V) h_c(V)(V - V_c)$$

where c denotes the current type ($c \in NaT, NaP, Kf, Ks$), where T, P, f, and s stand for 'Transient', 'Persistent', 'fast', and 'slow' correspondingly, p is the number of activation gates.

Activation and inactivation variables are governed by ($x \in m, h$):

$$\frac{dx}{dt}(V) = \frac{x_{c,\infty}(V) - x}{\tau_c(V)}$$

where the steady states $x_{c,\infty}$ are defined as:

$$x_{c,\infty}(V) = \frac{1}{1 + \exp\left([V - V_{c,x,1/2}]/k_{c,x,1/2}\right)}$$

The parameters are given in Table 1.

		Activation			**Inactivation**		
Current	p	$V_{1/2,m}$ (mV)	k_m (mV)	τ_m (ms)	$V_{1/2,h}$ (mV)	k_h (mV)	τ_h (ms)
NaT	3	-29.13	-8.92	$0.13 + \frac{3.43}{1+\exp\left((V+45.35)/5.98\right)}$	-47	5	$0.36 + \exp\left(\frac{V+20.65}{-10.47}\right)$
NaP	1	-48.77	-3.68	1	$-$	$-$	$-$
Ks	4	-12.85	-19.91	$2.03 + \frac{1.96}{1+\exp\left((V-29.83)/3.32\right)}$	-	-	-
Kf	4	-17.55	-7.27	$1.94 + \frac{2.66}{1+\exp\left((V-8.12)/7.96\right)}$	-45	6	$1.79 + \frac{515.8}{1+\exp\left((V+147.4)/28.66\right)}$

Table 1: Channel parameters for activation and inactivation of sodium and potassium channels.

Note 6. Similar parameters (small differences) is also given in [12].

1. There is only one Ih channel gene [1, 6]

2. Also known as DMIH (drosophila homologue of HCN channels)

4   R5 Model

Contents

- Wang 1994 model simulations

    - Blocking T-Type Ca^{2+} channel destroys LTS

    - Removing h current does not affect dynamics. H current is not necessary in the model

- Resting membrane potential of R5 is $\approx -49mV$ [15].

4.1   Model

4.2 Appendix

4.2.1 Reverse Engineering Wang 1994 Model

Reverse-Engineering Wang 1994

Stops activity :
- I_L
- I_L, I_R
- I_K
- I_K, I_R
- I_K, I_L
- I_K, I_L, I_R
- I_{Na}, I_L

- I_{Na}, I_L, I_R
- I_{Na}, I_K
- I_{Na}, I_K, I_R
- I_{Na}, I_K, I_R
- I_{Na}, I_K, I_L, I_R
- $I_{Na,P}, I_h, I_R$
- $I_{Na,P}, I_K$
- $I_{Na,P}, I_K, I_R$

- $I_{Na,P}, I_h, I_L$
- $I_{Na,P}, I_K, I_L, I_R$
- $I_{Na,P}, I_{Na}, I_K, I_R$

Oscillating:
- $I_{Na,P}$
- $I_{Na,P}, I_R$
- $I_{Na,P}, I_L$
- $I_{Na,P}, I_{Na}$

- $I_{Na,P}, I_{Na}, I_R$
- $I_{Na,P}, I_{Na}, I_L$
- $I_{Na,P}, I_{Na}, I_h$
- $I_{Na,P}, I_{Na}, I_K, I_R$
- $I_{Na,P}, I_{Na}, I_K, I_L$

LTS Like
Low amplitude
Weird
High amplitude

Bursting:
- I_R
- I_{Na}
- I_{Na}, I_R

→ $I_{Na,P}, I_L, I_K,$ and I_T are necessary & sufficient for bursting

→ I_T, I_L are necessary and sufficient for LTS

Inward $(I < 0)$: $I_T, I_{Na}, I_{Na,P}, I_R$

Outward $(I > 0)$: $I_K, I_L, (I_R)$

$I_{Na,P}$ — B
I_{Na} — T
I_h — B, T
I_L — B, LTS
I_T — B, LTS
I_h — ?

24

Figure 10

$I_{Na_p}: O; I_{Na}: B; I_K: O; I_L: O; I_h: B$
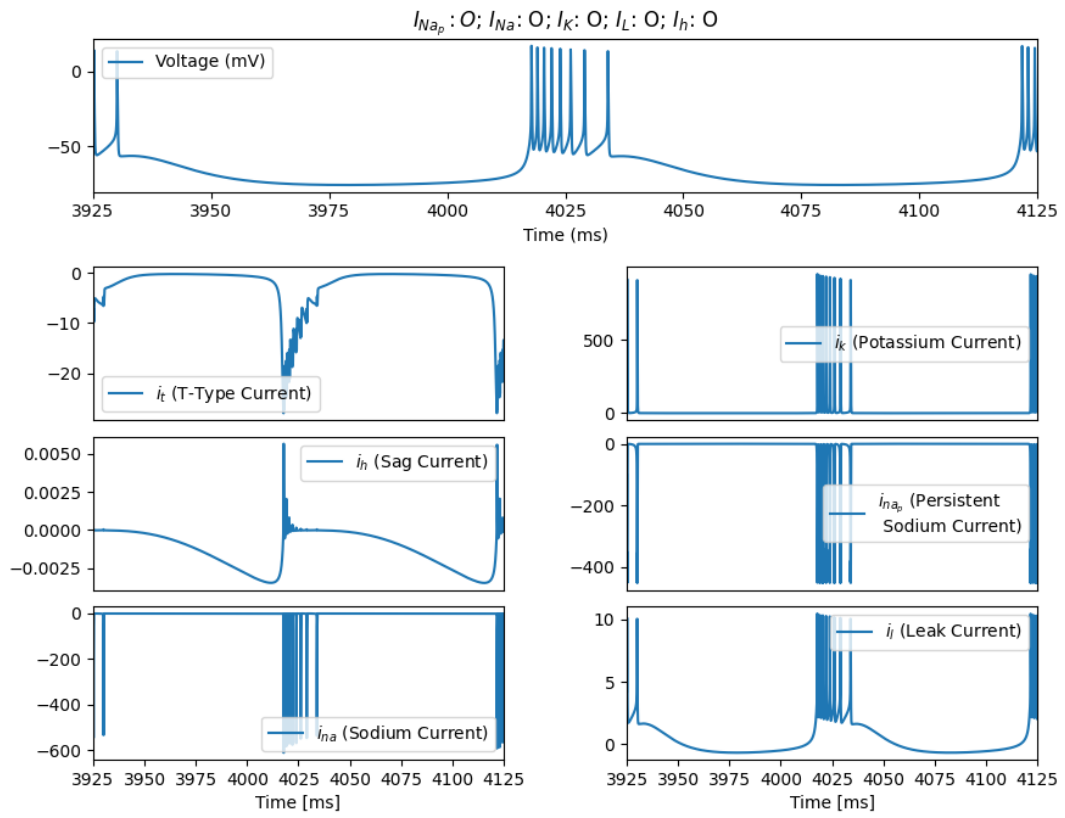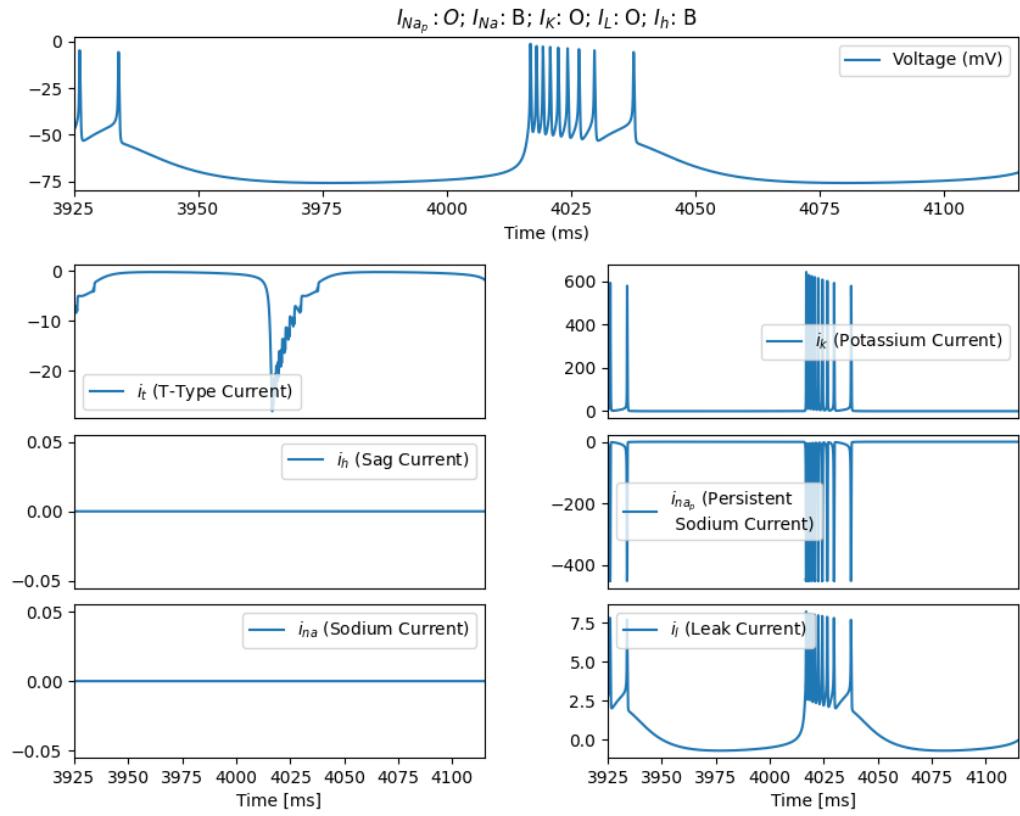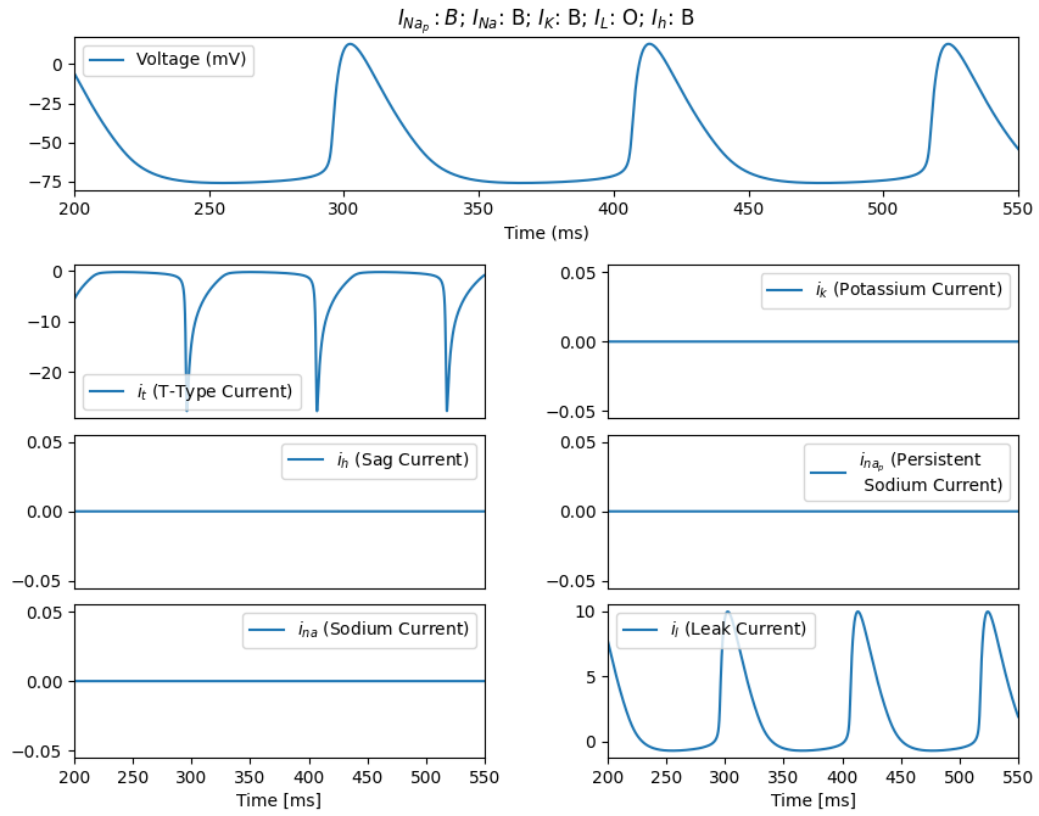
Figure 11

Figure 12

5   General Notes

Contents

5.1   Notes from Books/Papers

Note 7. [In this equation...] the time evolution depends only on the present state of the system, and is defined entirely by knowledge of the set of transition probabilities. Such systems are called *Markovian systems.*

5.2 Handwritten Notes

<u>Contents</u>

30

Ion Currents

Inside

Na^+ $(5-15\ mM)$

K^+ $(140\ mM)$

Cl^- $(4\ mM)$

Ca^{2+} $(0.1\mu M)$

A^- $(147\ mM)$

K^+K^+

$(Pump)$

$Na^+\ Na^+$
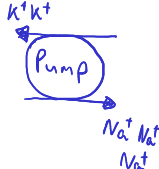Na^+

Outside

Na^+ $(145\ mM)$

K^+ $(5\ mM)$

Cl^- $(110\ mM)$

Ca^{2+} $(2.5-5\ mM)$

A^- $(25\ mM)$

Equilibrium potential:

$$E_{ion} = \frac{RT}{zF}\ ln\left[\frac{[Ion]_{out}}{[Ion]_{in}}\right]$$

Ionic current:

$$I_{ion} = g_{ion}(V - E_{ion})$$

$$E_K < E_{Cl} < V_{rest} < E_{Na} < E_{Ca}$$

Inward currents $(I_{Na}, I_{Ca} < 0)$ increase the membrane potential (depolarization); Outward currents $(I_K, I_{Cl} > 0)$ decrease it (hyperpolarization). I_{Cl} is called outward current even though the flow of Cl^- ions is inward; the ions bring negative charge inside the membrane, which is equivalent to positively charged ions leaving the cell, as in I_K.

$$C\dot{V} = I - I_{Na} - I_{Ca} - I_K - I_{Cl}$$

$-2-$

L, T, N, and P type Ca^{2+} channels
(Dayan & Abbott)

→ L-type Ca^{2+} currents are persistent as far as their voltage dependence is concerned, and they activate at a relatively high threshold. They inactivate due to a Ca^{2+}-dependent rather than voltage-dependent process. (Dayan & Abbott). Slowly inactivating, high-voltage activated (Suzuki et al 1989).

→ T-type Ca^{2+} currents have lower activation thresholds and are transient. (Dayan & Abbott). Rapidly inactivating, low-voltage activated. (Suzuki et al 1989)

→ N- and P-type Ca^{2+} conductances have intermediate thresholds and are transient and persistent, respectively. They may be responsible for the Ca^{2+} entry that causes the release of transmitter at presynaptic terminals (Dayan & Abbott). N-type channels are low-threshold, rapidly inactivating (Suzuki et al 1989).

-3-

Numerical Simulations

$$V(t + \Delta t) = V_\infty + (V(t) - V_\infty) \exp\left(-\frac{\Delta t}{\tau_V}\right) \qquad (1)$$

$$z(t + \Delta t) = z_\infty + (z(t) - z_\infty) \exp\left(-\frac{\Delta t}{\tau_z}\right) \qquad (2)$$

An efficient integration scheme for conductance-based models is to alternate using rule (1) to update the membrane potential and rule (2) to update all the gating variables. It is important to alternate the updating of V with that of the gating variables, rather than doing them all simultaneously, as this keeps the method accurate to second order in Δt. If Ca^{2+}-dependent conductances are included, the intracellular Ca^{2+} concentration should be computed simultaneously with the membrane potential. By alternating the updating, we mean that the membrane potential is computed at times $0, \Delta t, 2\Delta t, \ldots$ while the gating variables are computed at times $\Delta t/2, 3\Delta t/2, 5\Delta t/2, \ldots$ A discussion of the second-order accuracy of this scheme is given in Mascagni and Sherman (1998).

— 4 —

Fig. 9.12-13. Parameters (Izhikevich book)

$$C\dot{V} = I - \underset{L}{g}(V-E_L) - \underset{Na}{g}\,m_\infty(V)\left(V-E_{Na}\right) - \underset{K}{g}\,n(V-E_K) - \underset{M}{g}\,n_M(V-E_K)$$

(red annotations, left to right: 1 over C; 8 over g_L; -80 over E_L; 20 over g_{Na}; 60 over E_{Na}; 9 (from 10) over g_K; -90 over E_K; 5 over g_M; -90 over E_K)

fast ‖ slow

$$\dot{n} = (n_\infty - n)/\tau(V) = \cancel{1}\; 0.152$$

$$\dot{n}_M = (n_{M,\infty} - n_M)/\tau_M(V) = 20$$

$$m_\infty = \frac{1}{1+\exp\left[(V_{1/2}^{(m)} - V)/k^{(m)}\right]}$$

(below: -20 under $V_{1/2}^{(m)}$, 15 under $k^{(m)}$)

$$n_\infty = \frac{1}{1+\exp\left[(V_{1/2}^{(n)} - V)/k^{(n)}\right]}$$

(below: -25 under $V_{1/2}^{(n)}$, 5 under $k^{(n)}$)

$$n_{M,\infty} = \frac{1}{1+\exp\left[(V_{1/2}^{(M)} - V)/k^{(M)}\right]}$$

(below: -20 under $V_{1/2}^{(M)}$, 5 under $k^{(M)}$)

— 5 —

References

1. Chen, Z. & Wang, Z. Functional Study of Hyperpolarization Activated Channel (I h) in Drosophila Behavior. *Science China Life Sciences* **55,** 2–7. ISSN: 1674-7305, 1869-1889. http://link.springer.com/10.1007/s11427-012-4270-6 (2025) (Jan. 2012).

2. Coulter, D. A., Huguenard, J. R. & Prince, D. A. Calcium Currents in Rat Thalamocortical Relay Neurones: Kinetic Properties of the Transient, Low-Threshold Current. *The Journal of Physiology* **414,** 587–604. ISSN: 0022-3751. pmid: 2607443 (July 1989).

3. Destexhe, A., Contreras, D., Steriade, M., Sejnowski, T. J. & Huguenard, J. R. In Vivo, in Vitro, and Computational Analysis of Dendritic Calcium Currents in Thalamic Reticular Neurons. *The Journal of Neuroscience: The Official Journal of the Society for Neuroscience* **16,** 169–185. ISSN: 0270-6474. pmid: 8613783 (Jan. 1996).

4. Destexhe, A., Mainen, Z. F. & Sejnowski, T. J. Synthesis of Models for Excitable Membranes, Synaptic Transmission and Neuromodulation Using a Common Kinetic Formalism. *Journal of Computational Neuroscience* **1,** 195–230. ISSN: 0929-5313, 1573-6873. http://link.springer.com/10.1007/BF00961734 (2024) (Aug. 1994).

5. Frankenhaeuser, B. & Hodgkin, A. L. The Action of Calcium on the Electrical Properties of Squid Axons. *The Journal of Physiology* **137,** 218–244. ISSN: 0022-3751. pmid: 13449874 (July 11, 1957).

6. Gisselmann, G. *et al.* Variants of the Drosophila Melanogaster Ih-channel Are Generated by Different Splicing. *Insect Biochemistry and Molecular Biology* **35,** 505–514. ISSN: 09651748. https://linkinghub.elsevier.com/retrieve/pii/S0965174805000433 (2025) (May 2005).

7. Günay, C. *et al.* Distal Spike Initiation Zone Location Estimation by Morphological Simulation of Ionic Current Filtering Demonstrated in a Novel Model of an Identified Drosophila Motoneuron. *PLOS Computational Biology* **11** (ed Blackwell, K. T.) e1004189. ISSN: 1553-7358. https://dx.plos.org/10.1371/journal.pcbi.1004189 (2025) (May 15, 2015).

8. Huguenard, J. R. & McCormick, D. A. Simulation of the Currents Involved in Rhythmic Oscillations in Thalamic Relay Neurons. *Journal of Neurophysiology* **68,** 1373–1383. ISSN: 0022-3077, 1522-1598. https://www.physiology.org/doi/10.1152/jn.1992.68.4.1373 (2024) (Oct. 1, 1992).

9. Huguenard, J. R. & Prince, D. A. A Novel T-type Current Underlies Prolonged Ca(2+)-Dependent Burst Firing in GABAergic Neurons of Rat Thalamic Reticular Nucleus. *The Journal of Neuroscience: The Official Journal of the Society for Neuroscience* **12,** 3804–3817. ISSN: 0270-6474. pmid: 1403085 (Oct. 1992).

10. Izhikevich, E. M. *Dynamical Systems in Neuroscience: The Geometry of Excitability and Bursting* ISBN: 978-0-262-27607-8. https://direct.mit.edu/books/book/2589/Dynamical-Systems-in-NeuroscienceThe-Geometry-of (2024) (The MIT Press, July 21, 2006).

11. Jeong, K. *et al.* Ca-a1T, a Fly T-type Ca2+ Channel, Negatively Modulates Sleep. *Scientific Reports* **5,** 17893. ISSN: 2045-2322. pmid: 26647714. https://www.nature.com/articles/srep17893 (Dec. 9, 2015).

12. Lin, W.-H., Günay, C., Marley, R., Prinz, A. A. & Baines, R. A. Activity-Dependent Alternative Splicing Increases Persistent Sodium Current and Promotes Seizure. *The Journal of Neuroscience* **32,** 7267–7277. ISSN: 0270-6474, 1529-2401. https://www.jneurosci.org/lookup/doi/10.1523/JNEUROSCI.6042-11.2012 (2025) (May 23, 2012).

13. Lin, W.-H., Wright, D. E., Muraro, N. I. & Baines, R. A. Alternative Splicing in the Voltage-Gated Sodium Channel DmNa$_v$ Regulates Activation, Inactivation, and Persistent Current. *Journal of Neurophysiology* **102,** 1994–2006. ISSN: 0022-3077, 1522-1598. `https://www.ph ysiology.org/doi/10.1152/jn.00613.2009` (2025) (Sept. 2009).

14. Macleod, G. T., Hegström-Wojtowicz, M., Charlton, M. P. & Atwood, H. L. Fast Calcium Signals in *Drosophila* Motor Neuron Terminals. *Journal of Neurophysiology* **88,** 2659–2663. ISSN: 0022-3077, 1522-1598. `https://www.physiology.org/doi/10.1152/jn.00515.2002` (2024) (Nov. 1, 2002).

15. Raccuglia, D. *et al.* Network-Specific Synchronization of Electrical Slow-Wave Oscillations Regulates Sleep Drive in Drosophila. *Current Biology* **29,** 3611–3621.e3. ISSN: 09609822. `https://linkinghub.elsevier.com/retrieve/pii/S0960982219311200` (2025) (Nov. 2019).

16. Ravenscroft, T. A. *et al. Drosophila* Voltage-Gated Sodium Channels Are Only Expressed in Active Neurons and Are Localized to Distal Axonal Initial Segment-like Domains. *The Journal of Neuroscience* **40,** 7999–8024. ISSN: 0270-6474, 1529-2401. `https://www.jneuro sci.org/lookup/doi/10.1523/JNEUROSCI.0142-20.2020` (2025) (Oct. 14, 2020).

17. Wang, X. J., Rinzel, J. & Rogawski, M. A. A Model of the T-type Calcium Current and the Low-Threshold Spike in Thalamic Neurons. *Journal of Neurophysiology* **66,** 839–850. ISSN: 0022-3077, 1522-1598. `https://www.physiology.org/doi/10.1152/jn.1991.66.3.839` (2024) (Sept. 1, 1991).

18. Wang, X.-J. Multiple Dynamical Modes of Thalamic Relay Neurons: Rhythmic Bursting and Intermittent Phase-Locking. *Neuroscience* **59,** 21–31. ISSN: 03064522. `https://linki nghub.elsevier.com/retrieve/pii/0306452294900957` (2024) (Mar. 1994).

19. Warmke, J. W. *et al.* Functional Expression of *Drosophila Para* Sodium Channels. *The Journal of General Physiology* **110,** 119–133. ISSN: 0022-1295, 1540-7748. `https://rupre ss.org/jgp/article/110/2/119/32121/Functional-Expression-of-Drosophila-par a-Sodium` (2025) (Aug. 1, 1997).